LOFAR beamshapes and their use in calibration and imaging

Sarod Yatawatta
September 10, 2009

Abstract

This document describes the derivation of the approximate analytical beam models for the LOFAR low band and high band antennas and its usage in calibration and correction of image plane effects.

1 Introduction

This document describes the derivation of the beams for the LOFAR low band antenna (LBA) and the high band antenna (HBA). The geometries of the LBA and HBA dipoles are given in Fig. 1 and Fig. 2 respectively. We assume both of these to be composed of linear, thin wire elements. Moreover, we assume the ground plane to be an infinite conducting plane.

Note the essential parameters in the dipole geometry are the height h, length L and the slants α, α_1, and α_2 for both the LBA and HBA geometries. Although the geometry is defined in rectangular coordinates (x, y, z), we derive the beam in spherical polar coordinates (r, θ, ϕ) where θ and ϕ are the declination (measured from the zenith) and the azimuth respectively.

This document is organized as follows: After an initial introduction to basic electromagnetic constants, we derive the vector magnetic potential of an infinitesimal dipole element. Next, using this, we derive the far field electric field intensity. Afterwards, assuming a sinusoidal current distribution along the dipole, we derive the far field electric field and hence the beamshape. Next, we derive the E-Jones matrix for the beam and move on to the derivation of the full measurement equation. Next we consider correction of images for the effect of the beam. Finally, we derive the station beam which uses multiple dipole elements.
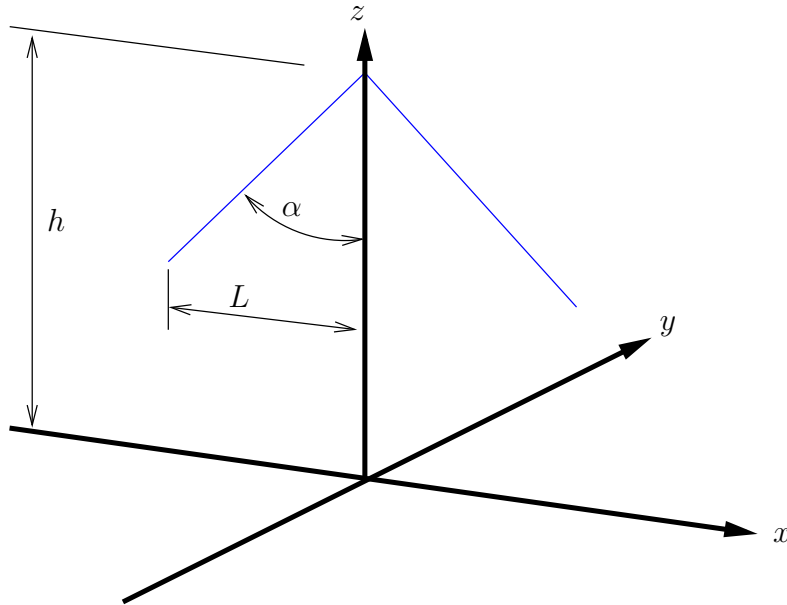

Figure 1: LBA X dipole geometry

2 Vector magnetic potential

Before we proceed, we define some fundamental parameters in electromagnetic theory (1),

$$c = \frac{1}{\sqrt{\mu_0 \epsilon_0}}, \ \omega = 2\pi f, \ k = \frac{\omega}{c} \tag{1}$$

where c is the speed of light in free space, f is the frequency, and k is the propagation constant. We consider an infinitesimal dipole with slant α (in xz plane) placed at the origin as in Fig. 3, with current I_0. The far
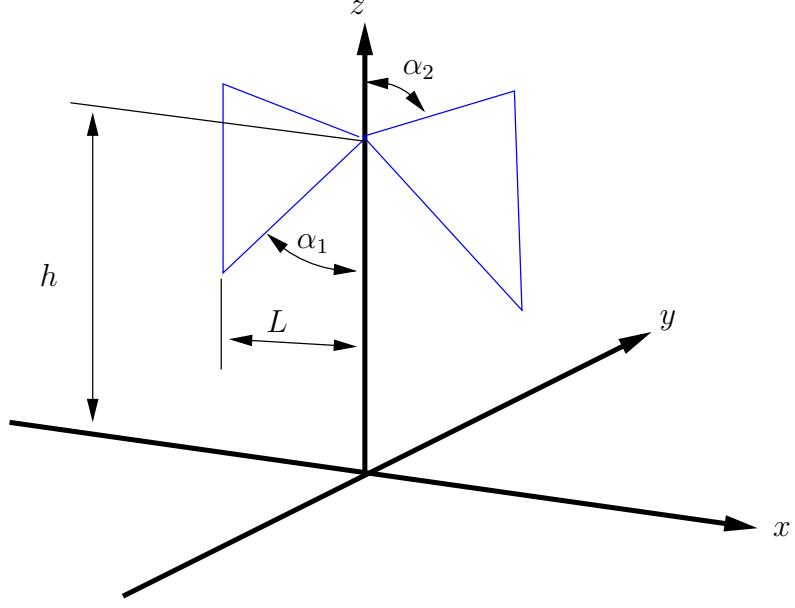
Figure 2: HBA X dipole geometry

field retarded magnetic potential is given by

$$A_x = \sin\alpha \frac{e^{-jkr}}{r}\frac{\mu I_0 d}{4\pi}, \ \ A_y = 0, \ \ A_z = \cos\alpha \frac{e^{-jkr}}{r}\frac{\mu I_0 d}{4\pi} \tag{2}$$
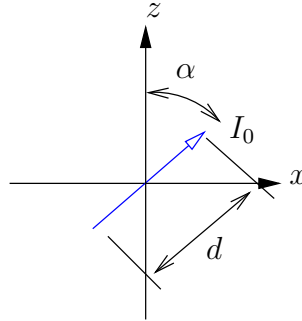
where d is the dipole length.

Figure 3: Infinitesimal dipole at origin

For a shift of origin of (ξ, η, ζ) in rectangular coordinates, the corresponding change in r in spherical polar coordinates is given in (3).

$$\bar{r} = r - (\xi\sin\theta\cos\phi + \eta\sin\theta\sin\phi + \zeta\cos\theta) \tag{3}$$

Next, we consider an infinitesimal dipole with an origin shift of $(a, 0, b)$ as in Fig. 4. Using (3), we get the far field retarded magnetic potential as in (4).

$$A_x = \sin\alpha \frac{e^{-jkr}}{r}\frac{\mu I_0 d}{4\pi}\exp(jk(a\sin\theta\cos\phi + b\cos\theta)), \ \ A_y = 0, \ \ A_z = \cos\alpha \frac{e^{-jkr}}{r}\frac{\mu I_0 d}{4\pi}\exp(jk(a\sin\theta\cos\phi + b\cos\theta)) \tag{4}$$

Note also that the conversion from (x, y, z) components to (r, θ, ϕ) components are given by (5).

$$\begin{bmatrix} A_r \\ A_\theta \\ A_\phi \end{bmatrix} = \begin{bmatrix} \sin\theta\cos\phi & \sin\theta\sin\phi & \cos\theta \\ \cos\theta\cos\phi & \cos\theta\sin\phi & -\sin\theta \\ -\sin\phi & \cos\phi & 0 \end{bmatrix} \begin{bmatrix} A_x \\ A_y \\ A_z \end{bmatrix} \tag{5}$$
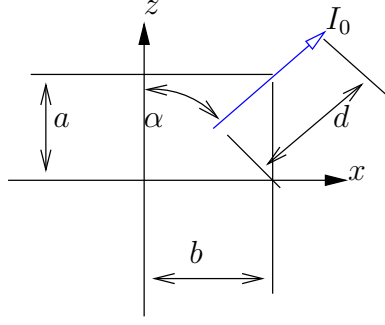
Figure 4: Infinitesimal dipole shifted by $(a, 0, b)$

Once we have found $\mathbf{A}$, we can derive the vector electric field $\mathbf{E}$ as in (6).

$$\mathbf{E} = -j\omega\mathbf{A} - \frac{j}{\omega\mu\epsilon}\nabla(\nabla \cdot \mathbf{A}) \tag{6}$$

Ignoring terms with r^{-2} or r^{-3}, we get the electric field terms as in (8). Note we have ignored the component in r because we know it to be identically zero for far field. For the far field, we also take the limit to get (7).

$$\lim_{r\to\infty} \frac{e^{-jkr}}{r} = -jk \tag{7}$$

$$
\begin{aligned}
E_\theta &= \frac{\mu I d}{4\pi}\omega k(\cos\alpha\sin\theta - \sin\alpha\cos\theta\cos\phi)\exp\left(jk(a\sin\theta\cos\phi + b\cos\theta)\right) \\
E_\phi &= \frac{\mu I d}{4\pi}\omega k(\sin\alpha\sin\phi)\exp\left(jk(a\sin\theta\cos\phi + b\cos\theta)\right)
\end{aligned}
\tag{8}
$$

We should remind ourselves that the electric field components in (8) are only due to a small length of the dipole. For the full contribution, we have to integrate over the dipole length. Finally, by superposition, we get the full contribution from all branches as a linear sum. In order to do so, we have to assume the current distribution along the dipole.

3 Current distributions

For a typical center fed, finite length dipole, we assume a sinusoidal current distribution with current being zero at the ends. This is directly applicable to the LBA model which has only an open conductor. However, for the HBA model this is not straight forward. In order to solve this, we follow the procedure given in [5]. In [5], each branch of the dipole is assumed to have a sinusoidal current distribution. In addition, the starting phase of the current was calculated from the preceding path length of the conductor.

In order to take into account the effects of the ground plane, we use image theory. The assumed current distribution for the LBA and HBA dipoles with their images due to ground plane is given in Fig. 5 and 6, respectively.

We first consider the LBA (as well as the horizontal branches of the HBA) as in Fig. 7.

$$\text{branch } 1 : \alpha \leftarrow \pi - \alpha, a = l, \ b = h - l/\tan\alpha, \ I = I_0\sin\left(\frac{k}{\sin\alpha}(L - l)\right), \ l \in [0, L] \tag{9}$$

$$\text{branch } 2 : \alpha \leftarrow \alpha, a = -l, \ b = h + l/\tan\alpha, \ I = I_0\sin\left(\frac{k}{\sin\alpha}(L + l)\right), \ l \in [-L, 0]$$

$$\text{branch } 3 : \alpha \leftarrow -\alpha, a = -l, \ b = -(h + l/\tan\alpha), \ I = I_0\sin\left(\frac{k}{\sin\alpha}(L + l)\right), \ l \in [-L, 0]$$

$$\text{branch } 4 : \alpha \leftarrow -\pi + \alpha, a = l, \ b = -(h - l/\tan\alpha), \ I = I_0\sin\left(\frac{k}{\sin\alpha}(L - l)\right), \ l \in [0, L]$$

If we consider the currents on the bottom vertical branches of the HBA (note the initial phase), as in Fig. 8, we get (10).

$$\text{branch } 1 : \alpha \leftarrow \pi/2, a = L, \ b = h - L/\tan\alpha_1 + l, \ I = e^{jkL/\sin\alpha_1}I_0\sin\left(k(L_1 - l)\right), \ l \in [0, L_1] \tag{10}$$
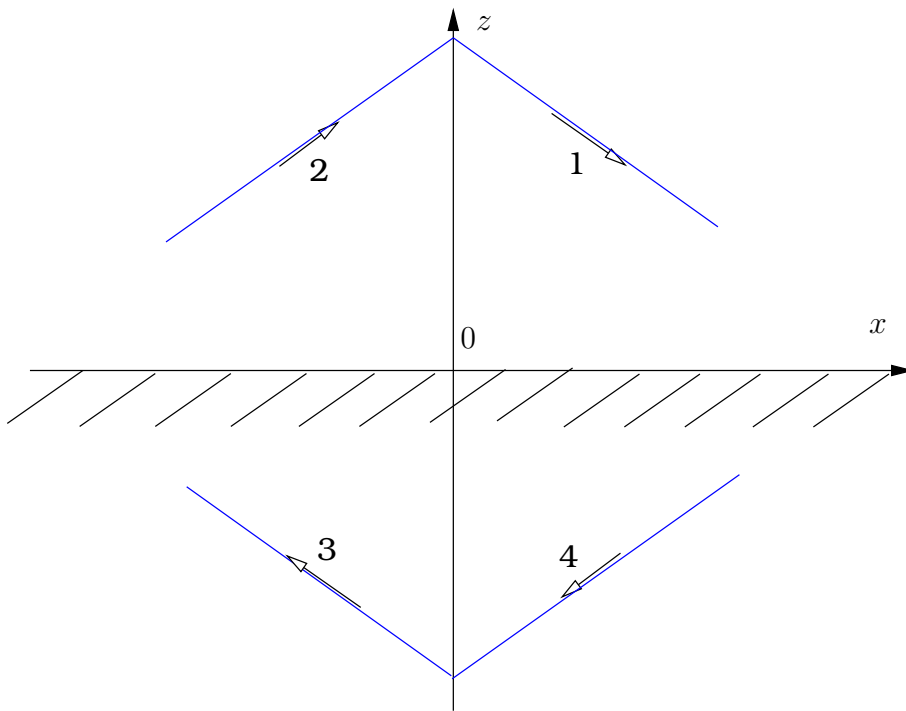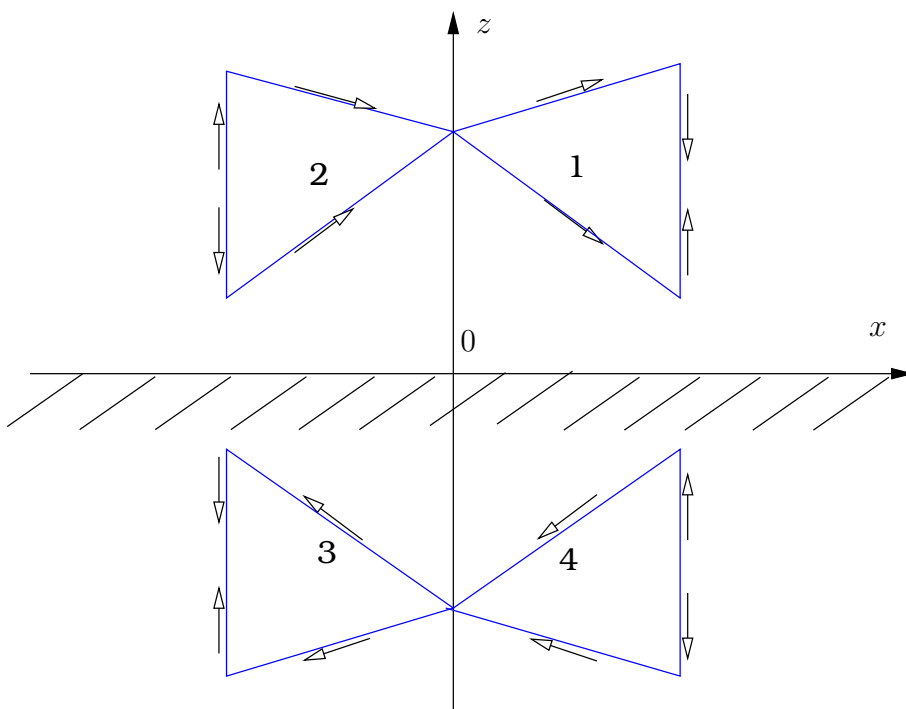
3

Figure 5: LBA dipole on infinite ground plane

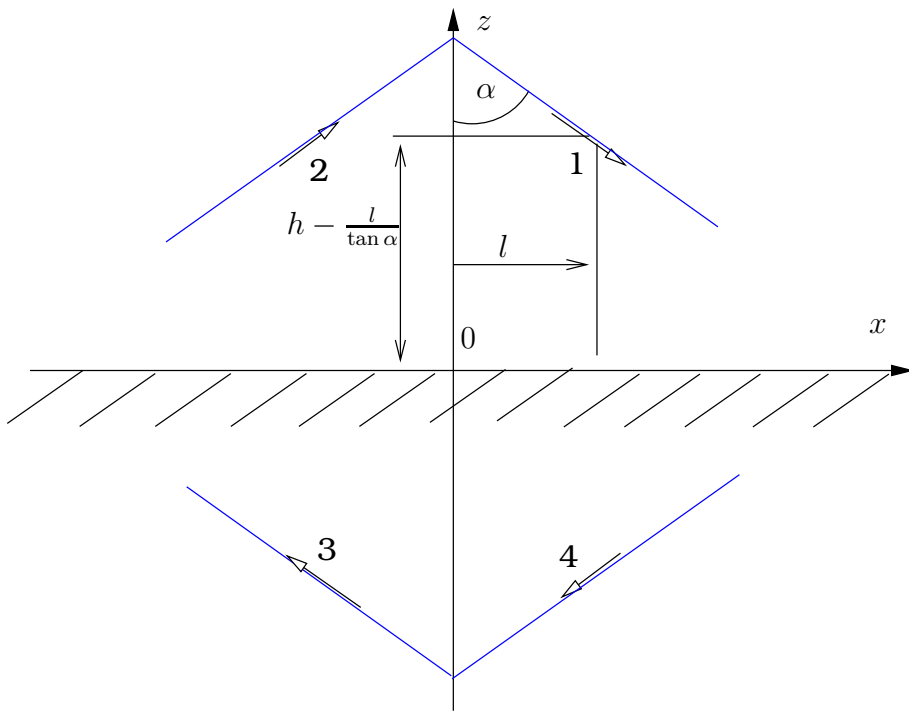Figure 6: HBA dipole on infinite ground plane

Figure 7: Currents on horizontal branches

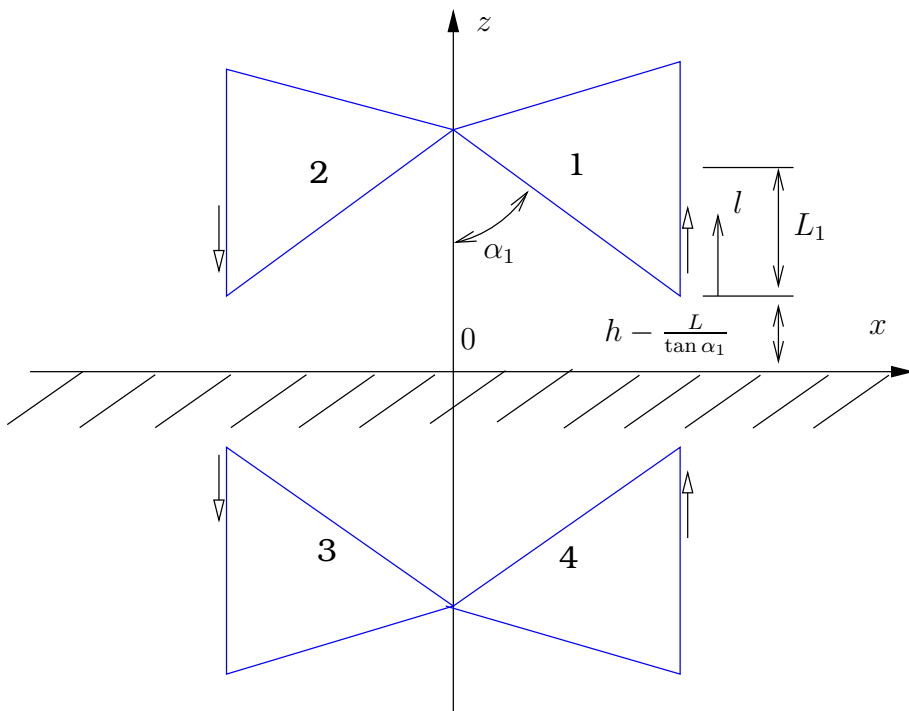Figure 8: Currents on bottom vertical branches

5

$$\text{branch } 2 : \alpha \leftarrow \pi/2, a = -L, \ b = h - L/\tan\alpha_1 + l, \ I = -e^{-jkL/\sin\alpha_1} I_0 \sin\big(k(L_1 - l)\big), \quad l \in [0, L_1]$$

$$\text{branch } 3 : \alpha \leftarrow \pi/2, a = -L, \ b = -(h - L/\tan\alpha_1 - l), \ I = -e^{jkL/\sin\alpha_1} I_0 \sin\big(k(L_1 + l)\big), \quad l \in [-L_1, 0]$$

$$\text{branch } 4 : \alpha \leftarrow \pi/2, a = L, \ b = -(h - L/\tan\alpha_1 - l), \ I = e^{-jkL/\sin\alpha_1} I_0 \sin\big(k(L_1 + l)\big), \quad l \in [-L_1, 0]$$
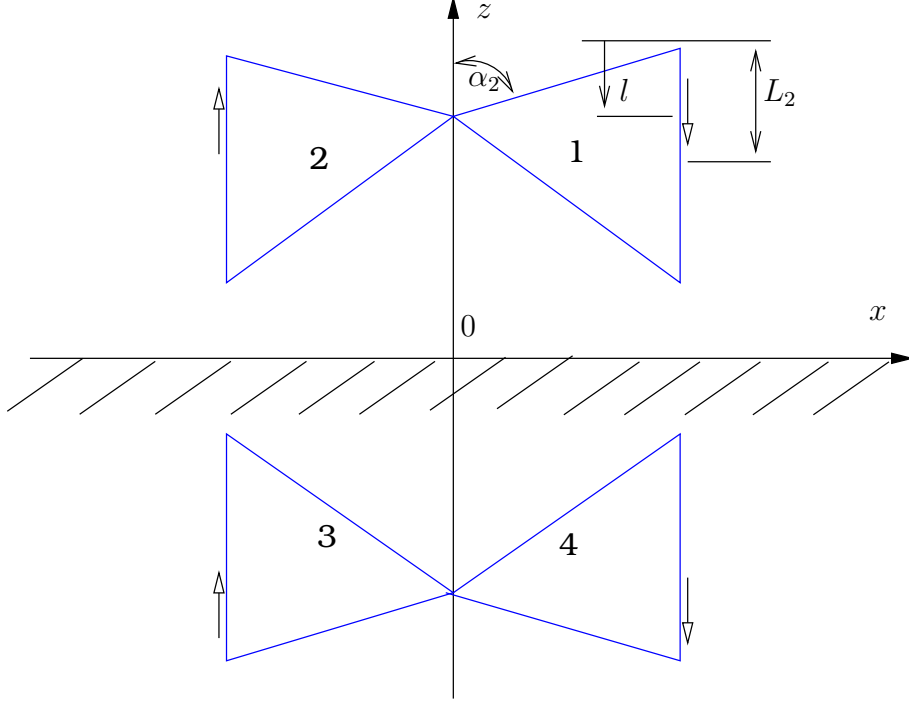

Figure 9: Currents on top vertical branches

Similarly, if we consider the currents on the top vertical branches of the HBA, as in Fig. 9, we get (11).

$$\text{branch } 1 : \alpha \leftarrow \pi/2, a = L, \ b = h + L/\tan\alpha_2 - l, \ I = -e^{jkL/\sin\alpha_2} I_0 \sin\big(k(L_2 - l)\big), \quad l \in [0, L_2] \tag{11}$$

$$\text{branch } 2 : \alpha \leftarrow \pi/2, a = -L, \ b = h + L/\tan\alpha_2 - l, \ I = e^{-jkL/\sin\alpha_2} I_0 \sin\big(k(L_2 - l)\big), \quad l \in [0, L_2]$$

$$\text{branch } 3 : \alpha \leftarrow \pi/2, a = -L, \ b = -(h + L/\tan\alpha_2 + l), \ I = e^{jkL/\sin\alpha_2} I_0 \sin\big(k(L_2 + l)\big), \quad l \in [-L_2, 0]$$

$$\text{branch } 4 : \alpha \leftarrow \pi/2, a = L, \ b = -(h + L/\tan\alpha_2 + l), \ I = -e^{-jkL/\sin\alpha_2} I_0 \sin\big(k(L_2 + l)\big), \quad l \in [-L_2, 0]$$

In order to find the electric field for the full length of the dipole, we need to use the integrals in (12).

$$
\begin{aligned}
\Gamma_+(A, B, k, L, \alpha) &\triangleq \int_0^L \exp\left(jk(Al + B)\right) \sin\left(\frac{k}{\sin\alpha}(L - l)\right) dl \\
&= \frac{-e^{jkB}}{k(A^2 - 1/\sin^2\alpha)} \left(\frac{e^{jkAL}}{\sin\alpha} - jA\sin(\frac{kL}{\sin\alpha}) - \frac{1}{\sin\alpha}\cos(\frac{kL}{\sin\alpha}) \right) \\
\Gamma_-(A, B, k, L, \alpha) &\triangleq \int_{-L}^0 \exp\left(jk(Al + B)\right) \sin\left(\frac{k}{\sin\alpha}(L + l)\right) dl \\
&= \frac{-e^{jkB}}{k(A^2 - 1/\sin^2\alpha)} \left(\frac{e^{-jkAL}}{\sin\alpha} + jA\sin(\frac{kL}{\sin\alpha}) - \frac{1}{\sin\alpha}\cos(\frac{kL}{\sin\alpha}) \right)
\end{aligned}
\tag{12}
$$

4 Electric field intensity

4.1 LBA and HBA horizontal branches

$$E_{\theta 1} = \frac{\mu I_0 \omega k}{4\pi}(-\cos\alpha_1 \sin\theta - \sin\alpha_1 \cos\theta \cos\phi) \tag{13}$$

6

$$\int_0^L \exp\left(jk(l\sin\theta\cos\phi + (h - l/\tan\alpha_1)\cos\theta)\right)\sin\left(\frac{k}{\sin\alpha_1}(L - l)\right)dl$$

$$= \frac{\mu I_0\omega k}{4\pi}(-\cos\alpha_1\sin\theta - \sin\alpha_1\cos\theta\cos\phi)$$

$$\Gamma_+(\sin\theta\cos\phi - \cos\theta/\tan\alpha_1, h\cos\theta, k, L, \alpha_1)$$

$$E_{\phi 1} = \frac{\mu I_0\omega k}{4\pi}(\sin\alpha_1\sin\phi) \tag{14}$$

$$\int_0^L \exp\left(jk(l\sin\theta\cos\phi + (h - l/\tan\alpha_1)\cos\theta)\right)\sin\left(\frac{k}{\sin\alpha_1}(L - l)\right)dl$$

$$= \frac{\mu I_0\omega k}{4\pi}(\sin\alpha_1\sin\phi)$$

$$\Gamma_+(\sin\theta\cos\phi - \cos\theta/\tan\alpha_1, h\cos\theta, k, L, \alpha_1)$$

$$E_{\theta 2} = \frac{\mu I_0\omega k}{4\pi}(\cos\alpha_1\sin\theta - \sin\alpha_1\cos\theta\cos\phi) \tag{15}$$

$$\int_{-L}^0 \exp\left(jk(-l\sin\theta\cos\phi + (h + l/\tan\alpha_1)\cos\theta)\right)\sin\left(\frac{k}{\sin\alpha_1}(L + l)\right)dl$$

$$= \frac{\mu I_0\omega k}{4\pi}(\cos\alpha_1\sin\theta - \sin\alpha_1\cos\theta\cos\phi)$$

$$\Gamma_-(-\sin\theta\cos\phi + \cos\theta/\tan\alpha_1, h\cos\theta, k, L, \alpha_1)$$

$$E_{\phi 2} = \frac{\mu I_0\omega k}{4\pi}(\sin\alpha_1\sin\phi) \tag{16}$$

$$\int_{-L}^0 \exp\left(jk(-l\sin\theta\cos\phi + (h + l/\tan\alpha_1)\cos\theta)\right)\sin\left(\frac{k}{\sin\alpha_1}(L + l)\right)dl$$

$$= \frac{\mu I_0\omega k}{4\pi}(\sin\alpha_1\sin\phi)$$

$$\Gamma_-(-\sin\theta\cos\phi + \cos\theta/\tan\alpha_1, h\cos\theta, k, L, \alpha_1)$$

$$E_{\theta 3} = \frac{\mu I_0\omega k}{4\pi}(\cos\alpha_1\sin\theta + \sin\alpha_1\cos\theta\cos\phi) \tag{17}$$

$$\int_{-L}^0 \exp\left(jk(-l\sin\theta\cos\phi - (h + l/\tan\alpha_1)\cos\theta)\right)\sin\left(\frac{k}{\sin\alpha_1}(L + l)\right)dl$$

$$= \frac{\mu I_0\omega k}{4\pi}(\cos\alpha_1\sin\theta + \sin\alpha_1\cos\theta\cos\phi)$$

$$\Gamma_-(-\sin\theta\cos\phi - \cos\theta/\tan\alpha_1, -h\cos\theta, k, L, \alpha_1)$$

$$E_{\phi 3} = \frac{\mu I_0\omega k}{4\pi}(-\sin\alpha_1\sin\phi) \tag{18}$$

$$\int_{-L}^0 \exp\left(jk(-l\sin\theta\cos\phi - (h + l/\tan\alpha_1)\cos\theta)\right)\sin\left(\frac{k}{\sin\alpha_1}(L + l)\right)dl$$

$$= \frac{\mu I_0\omega k}{4\pi}(-\sin\alpha_1\sin\phi)$$

$$\Gamma_-(-\sin\theta\cos\phi - \cos\theta/\tan\alpha_1, -h\cos\theta, k, L, \alpha_1)$$

$$E_{\theta 4} = \frac{\mu I_0\omega k}{4\pi}(-\cos\alpha_1\sin\theta + \sin\alpha_1\cos\theta\cos\phi) \tag{19}$$

$$\int_0^L \exp\left(jk(l\sin\theta\cos\phi - (h - l/\tan\alpha_1)\cos\theta)\right)\sin\left(\frac{k}{\sin\alpha_1}(L - l)\right)dl$$

$$= \frac{\mu I_0\omega k}{4\pi}(-\cos\alpha_1\sin\theta + \sin\alpha_1\cos\theta\cos\phi)$$

$$\Gamma_+(\sin\theta\cos\phi + \cos\theta/\tan\alpha_1, -h\cos\theta, k, L, \alpha_1)$$

$$E_{\phi 4} = \frac{\mu I_0 \omega k}{4\pi}(-\sin\alpha_1 \sin\phi) \tag{20}$$

$$\int_0^L \exp\left(jk(l\sin\theta\cos\phi - (h - l/\tan\alpha_1)\cos\theta)\sin\left(\frac{k}{\sin\alpha_1}(L-l)\right)\right) dl$$

$$= \frac{\mu I_0 \omega k}{4\pi}(-\sin\alpha_1 \sin\phi)$$

$$\Gamma_+(\sin\theta\cos\phi + \cos\theta/\tan\alpha_1, -h\cos\theta, k, L, \alpha_1)$$

We can also derive the electric field components for the top horizontal branch of the HBA by using $\pi - \alpha_2$ for α_1 in the above formulae.

4.2   HBA bottom vertical branches

$$E_{\theta 1} = \frac{\mu I_0 \omega k}{4\pi}(\sin\theta)\exp(jk\frac{L}{\sin\alpha_1}) \tag{21}$$

$$\int_0^{L_1} \exp\left(jk(L\sin\theta\cos\phi + (h - L/\tan\alpha_1 + l)\cos\theta)\sin\left(k(L_1 - l)\right)\right) dl$$

$$= \frac{\mu I_0 \omega k}{4\pi}(\sin\theta)\exp(jk\frac{L}{\sin\alpha_1})\Gamma_+(\cos\theta, L\sin\theta\cos\phi + (h - L/\tan\alpha_1)\cos\theta, k, L_1, \pi/2)$$

$$E_{\theta 2} = \frac{\mu I_0 \omega k}{4\pi}(\sin\theta)(-\exp(-jk\frac{L}{\sin\alpha_1})) \tag{22}$$

$$\int_0^{L_1} \exp\left(jk(-L\sin\theta\cos\phi + (h - L/\tan\alpha_1 + l)\cos\theta)\sin\left(k(L_1 - l)\right)\right) dl$$

$$= \frac{\mu I_0 \omega k}{4\pi}(\sin\theta)(-\exp(-jk\frac{L}{\sin\alpha_1}))\Gamma_+(\cos\theta, -L\sin\theta\cos\phi + (h - L/\tan\alpha_1)\cos\theta, k, L_1, \pi/2)$$

$$E_{\theta 3} = \frac{\mu I_0 \omega k}{4\pi}(\sin\theta)(-\exp(jk\frac{L}{\sin\alpha_1})) \tag{23}$$

$$\int_{-L_1}^0 \exp\left(jk(-L\sin\theta\cos\phi - (h - L/\tan\alpha_1 - l)\cos\theta)\sin\left(k(L_1 + l)\right)\right) dl$$

$$= \frac{\mu I_0 \omega k}{4\pi}(\sin\theta)(-\exp(jk\frac{L}{\sin\alpha_1}))\Gamma_-(\cos\theta, -L\sin\theta\cos\phi - (h - L/\tan\alpha_1)\cos\theta, k, L_1, \pi/2)$$

$$E_{\theta 4} = \frac{\mu I_0 \omega k}{4\pi}(\sin\theta)(\exp(-jk\frac{L}{\sin\alpha_1})) \tag{24}$$

$$\int_{-L_1}^0 \exp\left(jk(L\sin\theta\cos\phi - (h - L/\tan\alpha_1 - l)\cos\theta)\sin\left(k(L_1 + l)\right)\right) dl$$

$$= \frac{\mu I_0 \omega k}{4\pi}(\sin\theta)(\exp(-jk\frac{L}{\sin\alpha_1}))\Gamma_-(\cos\theta, L\sin\theta\cos\phi - (h - L/\tan\alpha_1)\cos\theta, k, L_1, \pi/2)$$

4.3   HBA top vertical branches

$$E_{\theta 1} = \frac{\mu I_0 \omega k}{4\pi}(\sin\theta)(-\exp(jk\frac{L}{\sin\alpha_2})) \tag{25}$$

$$\int_0^{L_2} \exp\left(jk(L\sin\theta\cos\phi + (h + L/\tan\alpha_2 - l)\cos\theta)\sin\left(k(L_2 - l)\right)\right) dl$$

$$= \frac{\mu I_0 \omega k}{4\pi}(\sin\theta)(-\exp(jk\frac{L}{\sin\alpha_2}))\Gamma_+(-\cos\theta, L\sin\theta\cos\phi + (h + L/\tan\alpha_2)\cos\theta, k, L_2, \pi/2)$$

$$E_{\theta 2} = \frac{\mu I_0 \omega k}{4\pi}(\sin\theta)(\exp(-jk\frac{L}{\sin\alpha_2})) \tag{26}$$

$$\int_0^{L_2} \exp\left(jk(-L\sin\theta\cos\phi + (h + L/\tan\alpha_2 - l)\cos\theta)\sin\left(k(L_2 - l)\right)\right) dl$$

$$= \frac{\mu I_0 \omega k}{4\pi}(\sin\theta)(\exp(-jk\frac{L}{\sin\alpha_2}))\Gamma_+(-\cos\theta, -L\sin\theta\cos\phi + (h + L/\tan\alpha_2)\cos\theta, k, L_2, \pi/2)$$

$$|E_\theta| \qquad\qquad |E_\phi|$$

Figure 10: LBA Beam at 10 MHz

$$
\begin{aligned}
E_{\theta 3}= \;& \frac{\mu I_0 \omega k}{4\pi}(\sin\theta)(\exp(jk\frac{L}{\sin\alpha_2})) \\
& \int_{-L_2}^{0} \exp\left(jk(-L\sin\theta\cos\phi - (h + L/\tan\alpha_2 + l)\cos\theta)\sin\left(k(L_2 + l)\right)\right) dl \\
= \;& \frac{\mu I_0 \omega k}{4\pi}(\sin\theta)(\exp(jk\frac{L}{\sin\alpha_2}))\Gamma_-(-\cos\theta, -L\sin\theta\cos\phi - (h + L/\tan\alpha_2)\cos\theta, k, L_2, \pi/2)
\end{aligned}
\tag{27}
$$

$$
\begin{aligned}
E_{\theta 4}= \;& \frac{\mu I_0 \omega k}{4\pi}(\sin\theta)(-\exp(-jk\frac{L}{\sin\alpha_2})) \\
& \int_{-L_2}^{0} \exp\left(jk(L\sin\theta\cos\phi - (h + L/\tan\alpha_2 + l)\cos\theta)\sin\left(k(L_2 + l)\right)\right) dl \\
= \;& \frac{\mu I_0 \omega k}{4\pi}(\sin\theta)(-\exp(-jk\frac{L}{\sin\alpha_2}))\Gamma_-(-\cos\theta, L\sin\theta\cos\phi - (h + L/\tan\alpha_2)\cos\theta, k, L_2, \pi/2)
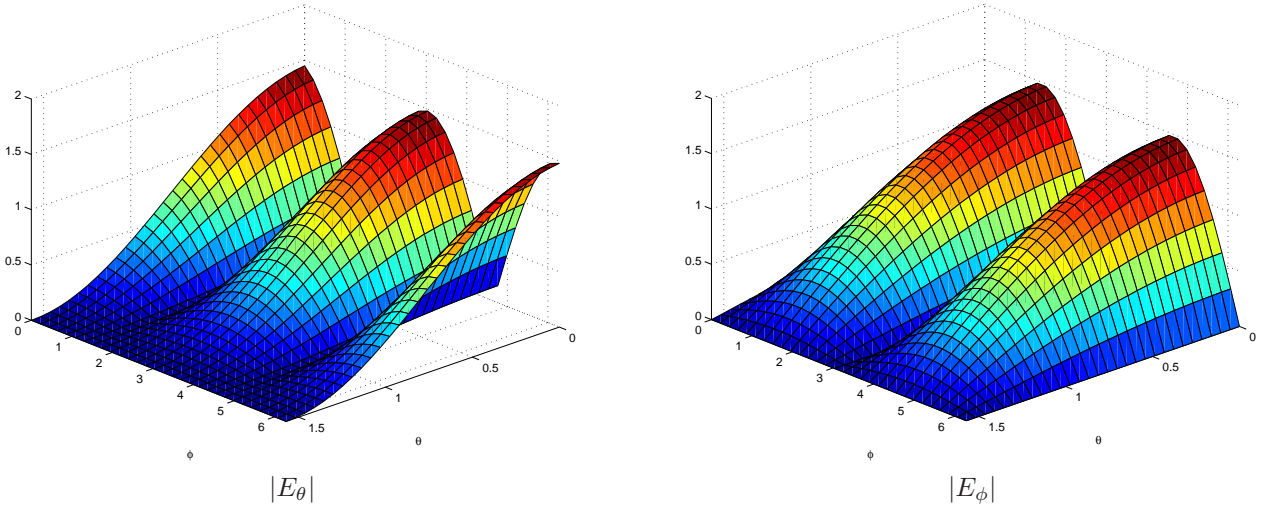\end{aligned}
\tag{28}
$$

The total electric field then is given by (29). Note that this is for the X dipole (we prefer to call it $\mathbf{E}_x$). For the Y dipole, we just need to substitute $\phi + \pi/2$ instead of ϕ in our formulae.

$$
\mathbf{E} = \sum_{i=1}^{4} \mathbf{E}_i, \quad \mathbf{E}_i = [0\ E_{\theta i}\ E_{\phi i}]^T
\tag{29}
$$

For the LOFAR LBA, we have $\alpha = 45\ deg$, $L = 1.38\sin\alpha\ m$ and $h = 1.706\ m$. The beamshapes at 10 MHz and 80 MHz are given in Fig. 10 and Fig. 11 respectively. For the LOFAR HBA, we have $\alpha_1 = 50\ deg$, $\alpha_2 = 80\ deg$, $L = 0.366\ m$ and $h = 0.45\ m$. The choice of L_1 and L_2 is purely arbitrary. In our case, we take L_1 and L_2 such that the top and bottom current paths have equal length. The beamshapes for this model at 100 MHz and 240 MHz are given in Fig. 12 and Fig. 13, respectively.

5   Station beamshape

In this section, we derive the beam shape of a station with multiple dipoles with beamforming. We follow the procedure given in [4]. Let us consider a plane wave approaching from the direction θ_0, ϕ_0 (spherical polar coordinates) onto a station with N dipole elements. The vector propagation constant, $\mathbf{k}_0$, for the approaching plane wave can be given as in (30), where ω_0 is the reference frequency (say $2\pi 60$ Mrad/s).

$$
\mathbf{k}_0 = \frac{\omega_0}{c}
\begin{bmatrix}
-\sin\theta_0 \cos\phi_0 \\
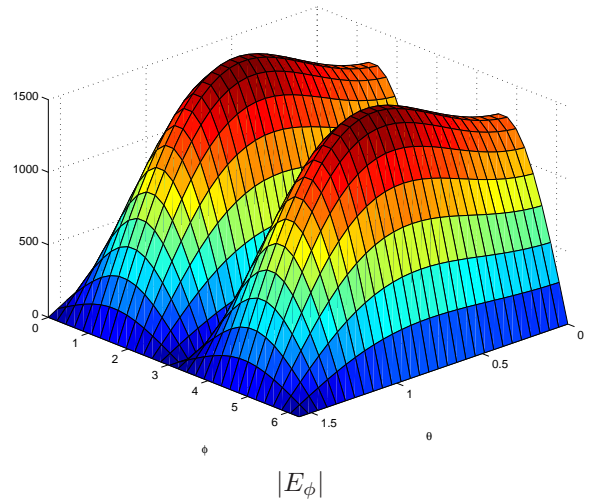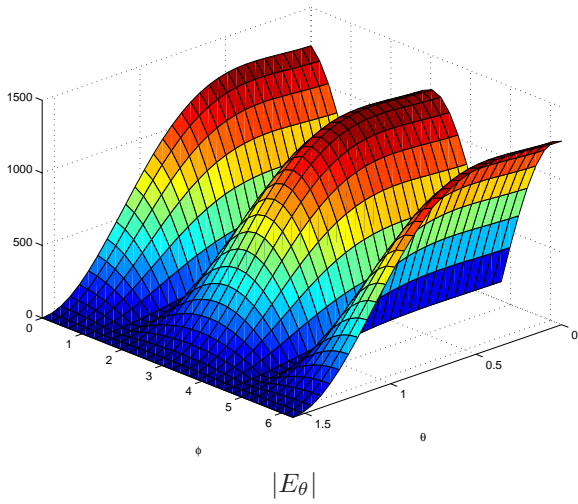-\sin\theta_0 \sin\phi_0 \\
-\cos\theta_0
\end{bmatrix}
\tag{30}
$$

9

$|E_\theta|$ $|E_\phi|$

Figure 11: LBA Beam at 80 MHz

$|E_\theta|$ $|E_\phi|$
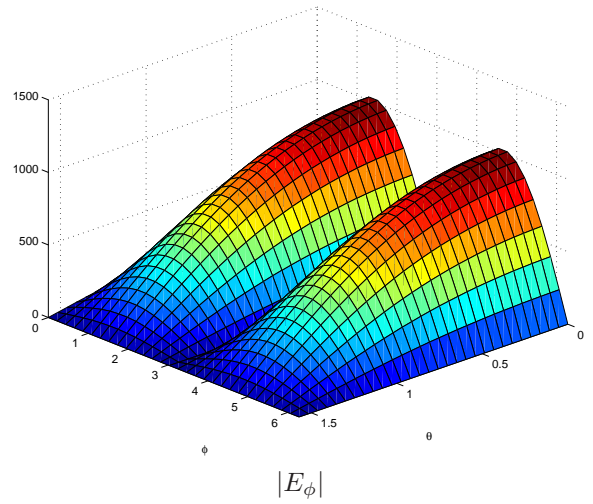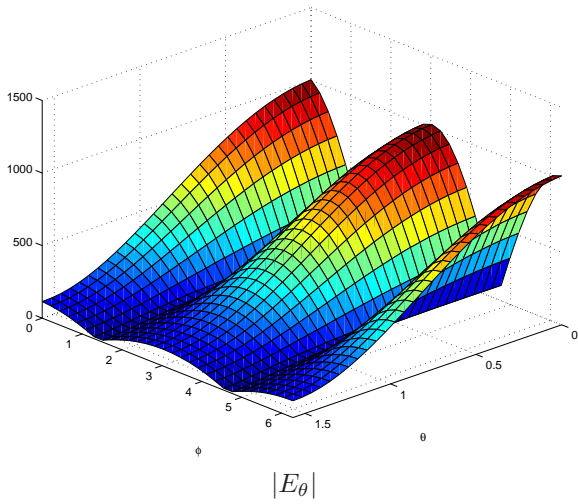
Figure 12: HBA Beam at 100 MHz

$|E_\theta|$ $|E_\phi|$
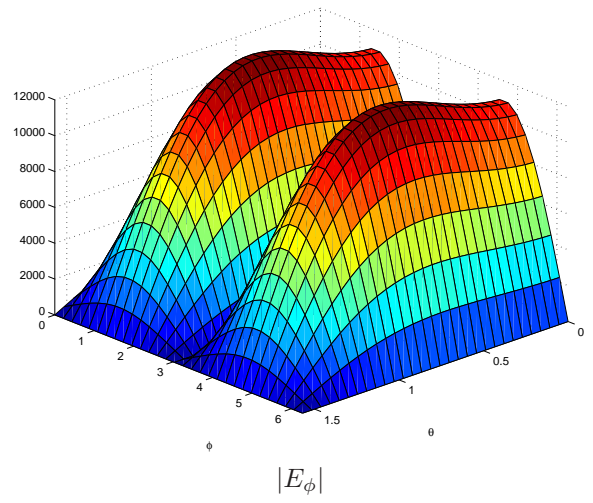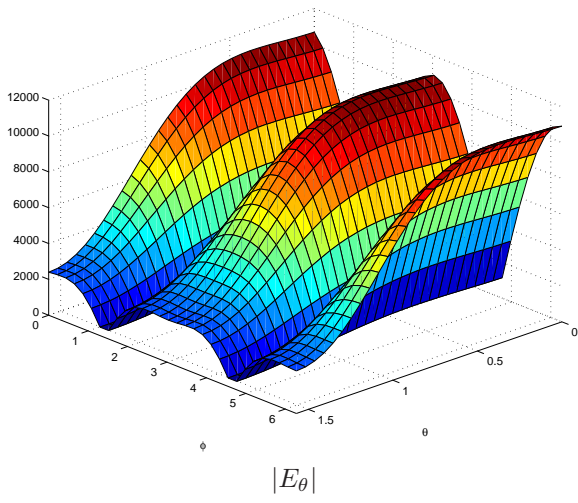
Figure 13: HBA Beam at 240 MHz

Let the rectangular coordinates of a dipole element in the station be given by $\mathbf{p}_n$ where n is the element index (31).

$$\mathbf{p}_n = \begin{bmatrix} p_x \\ p_y \\ p_z \end{bmatrix}, \quad n = 0, 1, \ldots, N-1 \tag{31}$$

Due to the spatial distribution of the elements, each has a different delay of reception of the plane wave. For instance, the delay at the n-th element τ_n can be given as in (32).

$$\tau_n = \frac{1}{\omega} \mathbf{k}_0^T \mathbf{p}_n \tag{32}$$

We define the array manifold vector $\mathbf{v_k}(\mathbf{k})$, for an arbitrary direction $\mathbf{k}$, as in (33).

$$\mathbf{v_k}(\mathbf{k}) = \begin{bmatrix} \exp(-j\mathbf{k}^T \mathbf{p}_0) \\ \exp(-j\mathbf{k}^T \mathbf{p}_1) \\ \vdots \\ \exp(-j\mathbf{k}^T \mathbf{p}_{N-1}) \end{bmatrix}, \quad \mathbf{k} = \frac{\omega}{c} \begin{bmatrix} -\sin\theta\cos\phi \\ -\sin\theta\sin\phi \\ -\cos\theta \end{bmatrix} \tag{33}$$

We assume a narrowband system and hence, the delay compensation is done just by using a phase shift for the signal of each element of the station. Now imagine we need to beam form in the direction (θ_0, ϕ_0). The vector of phase shifts for each element can be given as the weight vector $\mathbf{w}$ as in (34), where the delays τ_n are given in (32).

$$\mathbf{w} = \frac{1}{N} \begin{bmatrix} \exp(-j\omega\tau_0) \\ \exp(-j\omega\tau_1) \\ \vdots \\ \exp(-j\omega\tau_{N-1}) \end{bmatrix} \tag{34}$$

Then the frequency-wavenumber response for the station, $\Upsilon(\omega, \mathbf{k})$, is given by (35).

$$\Upsilon(\omega, \mathbf{k}) = \mathbf{w}^H \mathbf{v_k}(\mathbf{k}) \tag{35}$$

Assuming the elements have identical beams, given by $\mathbf{E}(\theta, \phi)$, the beamshape for the station is given by (36).

$$B(\omega; \theta, \phi) = \Upsilon(\omega, \mathbf{k})\mathbf{E}(\theta, \phi) \tag{36}$$

Note that at the phase centre, in (35) we get $\Upsilon(\omega, \mathbf{k}) = 1$ and therefore the beam shape evaluates to $B(\omega; \theta, \phi) = \mathbf{E}(\theta_0, \phi_0)$. In other words, at the phase centre, the station beam gain is equivalent to the gain of the dipole beam.

6 E-Jones matrix

In order to analyze the projection affecting polarized radiation, we refer to Fig. 14. We take the plane wave approaching the antenna to be linearly polarized, with components Λ_1 and Λ_2 in the directions $-\hat{\theta}$ and $\hat{\phi}$, respectively. As in [2, 1], we take the principle of reciprocity into account to find the components seen by the X,Y dipoles, i.e., V_x and V_y respectively.

If we use $\gamma = \pi/2 - \theta$ for elevation, and $\beta = \phi - \pi/4$ for azimuth, the root mean squared (RMS) voltages seen by the X and Y dipoles can be given as in (37) which summarizes our analysis in a neat and compact form. Note the field components in θ and ϕ directions are given by $\mathbf{E}_\theta(\gamma, \beta)$ and $\mathbf{E}_\phi(\gamma, \beta)$ respectively.

$$\begin{bmatrix} V_x \\ V_y \end{bmatrix} = \begin{bmatrix} \mathbf{E}_\theta(\gamma, \beta) & \mathbf{E}_\phi(\gamma, \beta) \\ \mathbf{E}_\theta(\gamma, \beta - \pi/2) & \mathbf{E}_\phi(\gamma, \beta - \pi/2) \end{bmatrix} \times \begin{bmatrix} \Lambda_1 \\ \Lambda_2 \end{bmatrix} \tag{37}$$

7 Measurement equation

We now consider the calibration of an interferometric array composed of dipoles as described above. This is directly applicable to the calibration of LOFAR CS1 . We start with (37). Consider the sky model to be only composed of N sources. Let us consider the visibilities seen on the baseline formed by station p and station

1.

Arbitrarily Polarized Radiation
Approaching

2.

Λ_1

Decomposition into Horizontal
and Vertical Components

Λ_2

3.

$E_{\theta x/y}\Lambda_1$

Attenuation by the X/Y beams

$E_{\phi x/y}\Lambda_2$

4.

V_x

by Reciprocity, current induction
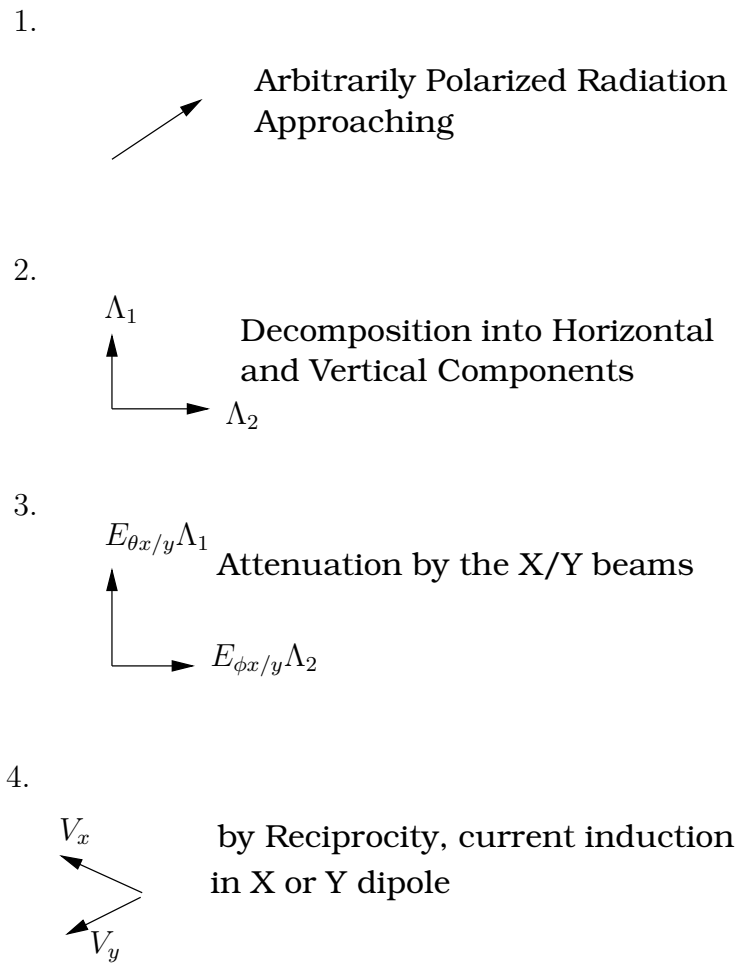in X or Y dipole

V_y

Figure 14: Attenuation of polarized radiation by the Beam

q. We also ignore leakage between the X and Y dipoles at each station. Then, the visibility seen on baseline pq can be expressed as in (38).

$$
\begin{bmatrix} XX & XY \\ YX & YY \end{bmatrix}_{pq} \tag{38}
$$

$$
= \begin{bmatrix} g_{11,p} & 0 \\ 0 & g_{22,p} \end{bmatrix} \mathbf{K}_p \left(\sum_{s=0}^{N-1} \begin{bmatrix} \mathbf{E}_{\theta,p}(\gamma,\beta) & \mathbf{E}_{\phi,p}(\gamma,\beta) \\ \mathbf{E}_{\theta,p}(\gamma,\beta-\pi/2) & \mathbf{E}_{\phi,p}(\gamma,\beta-\pi/2) \end{bmatrix}_s \times E\{ \begin{bmatrix} \Lambda_1 \\ \Lambda_2 \end{bmatrix} \times \begin{bmatrix} \Lambda_1 \\ \Lambda_2 \end{bmatrix}^H \}_s \right.
$$

$$
\times \left. \begin{bmatrix} \mathbf{E}_{\theta,q}(\gamma,\beta) & \mathbf{E}_{\phi,q}(\gamma,\beta) \\ \mathbf{E}_{\theta,q}(\gamma,\beta-\pi/2) & \mathbf{E}_{\phi,q}(\gamma,\beta-\pi/2) \end{bmatrix}_s^H \right) \mathbf{K}_q^H \begin{bmatrix} g_{11,q} & 0 \\ 0 & g_{22,q} \end{bmatrix}^H
$$

$$
= \mathbf{G}_p \mathbf{K}_p \left(\sum_{s=0}^{N-1} \mathbf{E}_{p,s}(\gamma,\beta) \mathbf{C}_s \mathbf{E}_{q,s}^H(\gamma,\beta) \right) \mathbf{K}_q^H \mathbf{G}_q^H
$$

$$
= \sum_{s=0}^{N-1} \mathbf{J}_{p,s} \mathbf{C}_s \mathbf{J}_{q,s}^H
$$

Note in (38), we have used subscripts p and q to denote terms belonging to stations p and q respectively. Moreover, we have absorbed the phase shift due to a source being off phase centre in Λ_1 and Λ_2 for simplicity. For an arbitrary source the coherency is given as in (39), which simplifies to a scalar matrix if $Q = U = V = 0$. Furthermore, I can be complex for a source off phase centre. For an unpolarized source, we have:

$$
E\{ \begin{bmatrix} \Lambda_1 \\ \Lambda_2 \end{bmatrix} \times \begin{bmatrix} \Lambda_1 \\ \Lambda_2 \end{bmatrix}^H \} = 0.5 \begin{bmatrix} I+Q & U-jV \\ U+jV & I-Q \end{bmatrix} = 0.5I \begin{bmatrix} 1 & 0 \\ 0 & 1 \end{bmatrix} \tag{39}
$$

After substitution of (39) back to (38), for a single (unpolarized) source, ($N = 1$), we get (40).

$$
\begin{bmatrix} XX & XY \\ YX & YY \end{bmatrix}_{pq} \tag{40}
$$

$$
= \frac{I}{2} \begin{bmatrix} g_{11,p} & 0 \\ 0 & g_{22,p} \end{bmatrix}
$$

$$
\times \begin{bmatrix} \mathbf{E}_{\theta,p}(\gamma,\beta)\mathbf{E}_{\theta,q}^\star(\gamma,\beta) + \mathbf{E}_{\phi,p}(\gamma,\beta)\mathbf{E}_{\phi,q}^\star(\gamma,\beta) & \mathbf{E}_{\theta,p}(\gamma,\beta)\mathbf{E}_{\theta,q}^\star(\gamma,\beta-\pi/2) + \mathbf{E}_{\phi,p}(\gamma,\beta)\mathbf{E}_{\phi,q}^\star(\gamma,\beta-\pi/2) \\ \mathbf{E}_{\theta,p}(\gamma,\beta-\pi/2)\mathbf{E}_{\theta,q}^\star(\gamma,\beta) + \mathbf{E}_{\phi,p}(\gamma,\beta-\pi/2)\mathbf{E}_{\phi,q}^\star(\gamma,\beta) & \mathbf{E}_{\theta,p}(\gamma,\beta-\pi/2)\mathbf{E}_{\theta,q}^\star(\gamma,\beta-\pi/2) + \mathbf{E}_{\phi,p}(\gamma,\beta-\pi/2)\mathbf{E}_{\phi,q}^\star(\gamma,\beta-\pi/2) \end{bmatrix}
$$

$$
\times \begin{bmatrix} g_{11,q}^\star & 0 \\ 0 & g_{22,q}^\star \end{bmatrix}
$$

8 Calibration

The essential objectives of LOFAR (CS1) calibration are

- Estimation of clock phases and electronic gains: $\mathbf{G}$ Jones matrices

- Estimation of beamshapes: $\mathbf{E}$ Jones matrices

- Removal of strongest sources: Cas A, Cyg A, Tau A, Vir A, Sun etc.

It should be noted here that for a single subband (bandwidth 0.16 MHz), the phase introduced by the beam is negligible compared to the phase introduced by the clock. Thus, in order to determine positions of discrete sources, the essential unknowns are the $\mathbf{G}$ Jones matrices. However, in order to accurately determine source fluxes, we need to estimate the $\mathbf{E}$ Jones matrices.

8.1 Single pass approach

Here we make an important assumption that the beams of all stations are identical (which we have to make in any case until we solve for the differences, which also enables us to drop the subscripts p and q). Then we can simplify (40) to get (41).

$$
\left[\begin{array}{cc} XX & XY \\ YX & YY \end{array}\right]_{pq} \tag{41}
$$

$$
= \frac{I}{2}\left[\begin{array}{cc} g_{11,p} & 0 \\ 0 & g_{22,p} \end{array}\right]
$$

$$
\times \left[\begin{array}{cc} |\mathbf{E}(\gamma,\beta)|^2 & \mathbf{E}_\theta(\gamma,\beta)\mathbf{E}_\theta^\star(\gamma,\beta-\pi/2) + \mathbf{E}_\phi(\gamma,\beta)\mathbf{E}_\phi^\star(\gamma,\beta-\pi/2) \\ \mathbf{E}_\theta(\gamma,\beta-\pi/2)\mathbf{E}_\theta^\star(\gamma,\beta) + \mathbf{E}_\phi(\gamma,\beta-\pi/2)\mathbf{E}_\phi^\star(\gamma,\beta) & |\mathbf{E}(\gamma,\beta-\pi/2)|^2 \end{array}\right]
$$

$$
\times \left[\begin{array}{cc} g_{11,q}^\star & 0 \\ 0 & g_{22,q}^\star \end{array}\right]
$$

Now let us consider solving for **J** Jones matrices (without any beam) for the visibilities in (41). Our measurement equation will be as in (42).

$$
\left[\begin{array}{cc} XX & XY \\ YX & YY \end{array}\right]_{pq} \tag{42}
$$

$$
= \frac{I}{2}\left[\begin{array}{cc} J_{11,p} & J_{12,p} \\ J_{21,p} & J_{22,p} \end{array}\right] \times \left[\begin{array}{cc} J_{11,q} & J_{12,q} \\ J_{21,q} & J_{22,q} \end{array}\right]^H
$$

Note that if we ignore the cross terms XY and YX in the solution process and assume the off diagonal terms of (42) to be zero, it reduces to (43).

$$
\begin{aligned}
XX &= \frac{I}{2}J_{11,p}J_{11,q}^\star = \frac{I}{2}g_{11,p}|\mathbf{E}(\gamma,\beta)|^2 g_{11,q}^\star \\
YY &= \frac{I}{2}J_{22,p}J_{22,q}^\star = \frac{I}{2}g_{22,p}|\mathbf{E}(\gamma,\beta-\pi/2)|^2 g_{22,q}^\star
\end{aligned} \tag{43}
$$

The solutions of (43) will yield us the true phase of g_{11} and g_{22} (upto a complex ambiguity), but not the amplitudes because of the beam. Nevertheless, we can use these solutions (i.e., J_{11} and J_{22}) to correct for the clock phase. This will also enable us to subtract the contribution of each source from the visibilities. On the other hand, if we try to solve for the full **J** Jones matrices in (42), the solutions will not give us the uv plane phase correction. So, in conclusion, without *prior knowledge of the beam*, the only alternative is to solve for the diagonal terms of the **J** Jones matrices only and use them for uv plane phase correction. Indeed, with full knowledge of the beam we can improve our solutions by solving for the full **J** Jones matrices.

The drawbacks of this approach are:

- Interaction of solutions of Cas A and Cyg A, even when Cas A has a high enough signal to noise ratio (SNR), the poor SNR of Cyg A solution would corrupt the residuals.

- The residuals are biased by the beam gain in direction of Cas A, (or Cyg A), depending on which solution is used to correct the residuals.

- Inherent assumption that the beams are identical.

- The solution differs from the true solution by a complex scalar for the X and Y system. After correction, this does not affect XX or YY, but it is remaining in XY and YX correlations. This is similar to the phase zero difference in WSRT. Thus the U and V polarizations are inaccurate.

8.2   Two pass approach

In the two pass approach, we need to have an a priori beam model. Thus, we can apply this to situations where the beams are not identical (i.e., with rotated dipoles). In the first pass, we estimate the **G** Jones matrices, using a pre calculated **E** Jones in (38). After correcting the visibilites using our estimated **G**, in the second pass, we peel off the strong sources (Cas A and Cyg A), without assuming any beam model, and using a full **J** Jones matrix for each source (per direction). The advantages of this approach are:

- No interaction of solutions, even when Cyg A is close to horizon

- In the second stage, we can solve for larger time intervals, thus giving a better SNR, improving the removal of Cyg A.

- We can peel off Cas A and Cyg A using full **J** Jones matrices.

- Unlike the single pass approach, the ambiguity for the X and Y system is the same (a complex scalar). Hence we do not have the phase zero difference problem. So all polarizations I,Q,U,V are accurate upto the beam model error.

However, there are some drawbacks of this approach:

- Requirement of an a priori beam model

- Need the accurate fluxes of sources in the model (especially Cas A to Cyg A flux ratio)

- Requires more computations

Not also that the solutions obtained in the second pass (i.e., the $\mathbf{J}$ matrices) should be identically equal to the $\mathbf{E}$ Jones matrices in the ideal case. However, this is affected by the a priori beam model we use in the first pass. Moreover, the ratio of the solutions in the directions of Cas A and Cyg A (say using Frobenius norm) should give us some idea of their flux ratio, subject to a systematic offset introduced by the beam.

8.3   The Holy Grail approach

This approach does not assume an a priori beam model. In this approach, we first solve for the full J Jones for each source in our model. Note from (38) that we can factor

$$\mathbf{J}_{p,s} = \mathbf{G}_p \mathbf{E}_{p,s}(\gamma, \beta), \quad p \in [0, M-1], \quad s \in [0, N-1] \tag{44}$$

For N stations, and for M sources, we have NM solutions for $\mathbf{J}$ Jones. Moreover, these are a product of N $\mathbf{G}$ Jones matrices and M $\mathbf{E}$ Jones matrices, assuming identical beamshapes. If we can find this unique factorization, we can recover both clock phaces as well as the true beamshapes. The factorization can be found using alternating least squares:

$$
\begin{bmatrix}
\mathbf{E}_0^T(\gamma, \beta) \otimes \mathbf{I} \\
\mathbf{E}_1^T(\gamma, \beta) \otimes \mathbf{I} \\
\vdots \\
\mathbf{E}_{N-1}^T(\gamma, \beta) \otimes \mathbf{I}
\end{bmatrix}
vec(\mathbf{G}_p) =
\begin{bmatrix}
vec(\mathbf{J}_{p,0}) \\
vec(\mathbf{J}_{p,1}) \\
\vdots \\
vec(\mathbf{J}_{p,N-1})
\end{bmatrix}
\tag{45}
$$

$$
\begin{bmatrix}
\mathbf{I} \otimes \mathbf{G}_0 \\
\mathbf{I} \otimes \mathbf{G}_1 \\
\vdots \\
\mathbf{I} \otimes \mathbf{G}_{M-1}
\end{bmatrix}
vec(\mathbf{E}_s(\gamma, \beta)) =
\begin{bmatrix}
vec(\mathbf{J}_{0,s}) \\
vec(\mathbf{J}_{1,s}) \\
\vdots \\
vec(\mathbf{J}_{M-1,s})
\end{bmatrix}
\tag{46}
$$

By solving (45) and (46) alternatively, we can converge to a solution. However, matrix factorization always results in a unitary ambiguity. Once we have the $\mathbf{J}$ Jones solutions, we need some a priori knowledege to remove this ambiguity. Current calibration software does not have this capability yet. Unlike the previous two cases where we only have a scalar ambiguity, thie methods introduces a matrix ambiguity, which can only be resolved by using external calibrators.

9   Correction for the beam

Let us assume that we have used the solutions of (43) in the direction of a particular source to correct the residual data. However, this does not correct for the effect of the beam, which is an image plane effect. For instruments such as WSRT, where the beam remains stationary with respect to the image, the correction can be applied after the final image for the full observation has been made.

However, for LOFAR, this approach fails because the beam moves with respect to the image (or vice versa). Let us consider the correction of an image with sufficiently small integration time such that we can assume the beam remains constant (in reality this will only hold for a snapshot image). We also assume the beams are identical for all stations. Note that as we see later, we do not need to make snapshot images for correction of Stokes I images, in other words, for Stokes I, we can use the whole integration time for imaging and correct for the beam withot making snapshots or facet images.

Let γ_0, β_0 be the elevation and azimuth of the source whose solution was used to correct the residual data at the time of the snapshot (e.g. the phace centre). Then, we have the solutions as given by (47) for single pass approach and as given by (48) for the two pass approach.

$$
\hat{\mathbf{G}}_p =
\begin{bmatrix}
\hat{g}_{11,p} & 0 \\
0 & \hat{g}_{22,p}
\end{bmatrix}
\approx
\begin{bmatrix}
g_{11,p}|\mathbf{E}(\gamma_0, \beta_0)| & 0 \\
0 & g_{22,p}|\mathbf{E}(\gamma_0, \beta_0 - \pi/2)|
\end{bmatrix}
\tag{47}
$$

$$\hat{\mathbf{G}}_p = \begin{bmatrix} \hat{g}_{11,p} & 0 \\ 0 & \hat{g}_{22,p} \end{bmatrix} \approx \begin{bmatrix} g_{11,p} & 0 \\ 0 & g_{22,p} \end{bmatrix} \tag{48}$$

Let us only consider the case when we have (47) as our solution because the alternative case is simpler. Let γ,β be the elevation and azimuth of an arbitrary pixel on the snapshot that we wish to correct for the beam. Let us define $\mathbf{C}$ and $\hat{\mathbf{C}}(\gamma,\beta)$ to be the true and estimated coherencies respectively of the pixel we are concerned with as in (49). Note that the estimated coherency depends on the patricular values of γ,β when the snapshot was made. The estimated and true full Stokes parameter values are given by $\hat{I},\hat{Q},\hat{U}$ and $\hat{V}$ and I,Q,U and V respectively.

$$\mathbf{C} \triangleq 0.5 \begin{bmatrix} I+Q & U+jV \\ U-jV & I-Q \end{bmatrix}, \quad \hat{\mathbf{C}}(\gamma,\beta) \triangleq 0.5 \begin{bmatrix} \hat{I}+\hat{Q} & \hat{U}+j\hat{V} \\ \hat{U}-j\hat{V} & \hat{I}-\hat{Q} \end{bmatrix} \tag{49}$$

We also assume we have made full polarization images and let the The corrected visibilities for baseline pq using the solution in (47) at that pixel can be given by (50), where we have used (38).

$$\hat{\mathbf{G}}_p^{-1} \begin{bmatrix} XX & XY \\ YX & YY \end{bmatrix}_{pq} \hat{\mathbf{G}}_q^{-H} \tag{50}$$

$$= 0.5 \begin{bmatrix} \hat{I}+\hat{Q} & \hat{U}+j\hat{V} \\ \hat{U}-j\hat{V} & \hat{I}-\hat{Q} \end{bmatrix}$$

$$= \begin{bmatrix} 1/|\mathbf{E}(\gamma_0,\beta_0)| & 0 \\ 0 & 1/|\mathbf{E}(\gamma_0,\beta_0-\pi/2)| \end{bmatrix} \times \begin{bmatrix} \mathbf{E}_\theta(\gamma,\beta) & \mathbf{E}_\phi(\gamma,\beta) \\ \mathbf{E}_\theta(\gamma,\beta-\pi/2) & \mathbf{E}_\phi(\gamma,\beta-\pi/2) \end{bmatrix} \times 0.5 \begin{bmatrix} I+Q & U+jV \\ U-jV & I-Q \end{bmatrix}$$

$$\times \begin{bmatrix} \mathbf{E}_\theta(\gamma,\beta) & \mathbf{E}_\phi(\gamma,\beta) \\ \mathbf{E}_\theta(\gamma,\beta-\pi/2) & \mathbf{E}_\phi(\gamma,\beta-\pi/2) \end{bmatrix}^H \times \begin{bmatrix} 1/|\mathbf{E}(\gamma_0,\beta_0)| & 0 \\ 0 & 1/|\mathbf{E}(\gamma_0,\beta_0-\pi/2)| \end{bmatrix}$$

Using (49), we can rewrite (50) in compact form as

$$\hat{\mathbf{C}}(\gamma,\beta) = \mathbf{\Pi}(\gamma,\beta)\mathbf{C}\mathbf{\Pi}(\gamma,\beta)^H \tag{51}$$

where $\mathbf{\Pi}(\gamma,\beta)$ is given by (52).

$$\mathbf{\Pi}(\gamma,\beta) \triangleq \begin{bmatrix} |\mathbf{E}(\gamma_0,\beta_0)| & 0 \\ 0 & |\mathbf{E}(\gamma_0,\beta_0-\pi/2)| \end{bmatrix}^{-1} \times \begin{bmatrix} \mathbf{E}_\theta(\gamma,\beta) & \mathbf{E}_\phi(\gamma,\beta) \\ \mathbf{E}_\theta(\gamma,\beta-\pi/2) & \mathbf{E}_\phi(\gamma,\beta-\pi/2) \end{bmatrix} \tag{52}$$

By inverting (51), we can get the full Stokes parameters for pixel at (γ,β), after correcting for the beam. However, for longer integration time, things become more complicated. Let $\hat{\mathbf{C}}$ be the coherency for the full observation as given in (53).

$$\hat{\mathbf{C}} = \sum_{\gamma,\beta} \hat{\mathbf{C}}(\gamma,\beta) = \sum_{\gamma,\beta} \left(\mathbf{\Pi}(\gamma,\beta)\mathbf{C}\mathbf{\Pi}(\gamma,\beta)^H \right) \neq \sum_{\gamma,\beta} \left(\mathbf{\Pi}(\gamma,\beta) \right) \mathbf{C} \sum_{\gamma,\beta} \left(\mathbf{\Pi}(\gamma,\beta)^H \right) \tag{53}$$

We see from (53) that for longer integration, we cannot apply the integrated beam to recover the true coherency. However, if we are only concerned with Stokes I value at the given pixel (i.e. we assume sources to be unpolarized), we can indeed do this. We use the fact that for an unpolarized source, $\mathbf{C} = I\mathbf{I}$, where $\mathbf{I}$ is an identity. The proof is given in (54).

$$\begin{aligned} \hat{I} &= \text{trace}(\hat{\mathbf{C}}) \\ &= \text{trace}(\sum_{\gamma,\beta} \hat{\mathbf{C}}(\gamma,\beta)) \\ &= \text{trace}(\sum_{\gamma,\beta} \left(\mathbf{\Pi}(\gamma,\beta)\mathbf{C}\mathbf{\Pi}(\gamma,\beta)^H \right)) \\ &= \sum_{\gamma,\beta} \left(\text{trace}(\mathbf{\Pi}(\gamma,\beta)\mathbf{C}\mathbf{\Pi}(\gamma,\beta)^H) \right) \\ &= \sum_{\gamma,\beta} \left(\text{trace}(\mathbf{C}\mathbf{\Pi}(\gamma,\beta)^H\mathbf{\Pi}(\gamma,\beta)) \right) \\ &= \text{trace}(\mathbf{C}\sum_{\gamma,\beta} \left(\mathbf{\Pi}(\gamma,\beta)^H\mathbf{\Pi}(\gamma,\beta) \right)) \\ &= I\,\text{trace}(\sum_{\gamma,\beta} \left(\mathbf{\Pi}(\gamma,\beta)^H\mathbf{\Pi}(\gamma,\beta) \right)) \end{aligned} \tag{54}$$

We can simplify our correction in (51) even further if we know a priori the sources are unpolarized. Notice that both $\mathbf{C}$ and $\hat{\mathbf{C}}$ are Hermitian. So we see (51) as the eigenvalue decomposition of $\hat{\mathbf{C}}$ (for a Hermitian matrix, the eigenvalues are real and the eigenvectors are orthonormal). So, without knowing the beam itself, we can recover Stokes I flux for an unpolarized pixel. This can also be used for verification of existing beam models.

10 Flux estimation

In this section we consider the estimation of flux densities of the sources in our sky model, in particular the ones in the A team. We start from (38) and consider perfect uv plane calibration. The observed data $\mathbf{V}_{pq}$ is given by (55) and assuming perfect calibration, ignoring the phase term, we get the corrected data $\tilde{\mathbf{V}}_{pq}$ for the interferometer pq as in (56).

$$\mathbf{V}_{pq} = \mathbf{G}_p \mathbf{K}_p \Big(\sum_{s=0}^{N-1} \mathbf{E}_{p,s}(\gamma,\beta) \mathbf{C}_s \mathbf{E}_{q,s}^H(\gamma,\beta) \Big) \mathbf{K}_q^H \mathbf{G}_q^H \tag{55}$$

$$\tilde{\mathbf{V}}_{pq} = (\mathbf{K}_p)^{-1}(\mathbf{G}_p)^{-1}\mathbf{V}_{pq}(\mathbf{G}_q)^{-H}(\mathbf{K}_q)^{-H} = \Big(\sum_{s=0}^{N-1} \mathbf{E}_{p,s}(\gamma,\beta) \mathbf{C}_s \mathbf{E}_{q,s}^H(\gamma,\beta) \Big) \tag{56}$$

In order to estimate fluxes, we need information of the beam or in other words the E-Jones matrix. However, in reality we only have a model which always has some error. There are basically two ways of estimating the flux as well as the beamshape. The obvious method is to find them both using uv plane data. The other way is to use snapshot images.

10.1 Direct method

If the true E-Jones is given by $\tilde{\mathbf{E}}_{p,s}(\gamma,\beta)$, let us relate this to the value that we model, $\mathbf{E}_{p,s}(\gamma,\beta)$, as in (57).

$$\tilde{\mathbf{E}}_{p,s}(\gamma,\beta) = \mathbf{E}_{p,s}(\gamma,\beta)(1+\varepsilon_s(\gamma)), \quad 0 \leq \gamma \leq \pi/2 \tag{57}$$

In (57), we assume the error $\varepsilon_s(\gamma)$ for a given source s is real and is only dependent on the elevation γ. The estimate of the coherencies $\tilde{\mathbf{C}}_s$ is related to the true coherencies $\mathbf{C}_s$ as in (58), assuming that the solver converges to the optimal value.

$$\sum_{s=0}^{N-1} \tilde{\mathbf{E}}_{p,s} \mathbf{C}_s \tilde{\mathbf{E}}_{q,s}^H = \sum_{s=0}^{N-1} (1+\varepsilon_s(\gamma))^2 \mathbf{E}_{p,s} \mathbf{C}_s \mathbf{E}_{q,s}^H = \sum_{s=0}^{N-1} \mathbf{E}_{p,s} \tilde{\mathbf{C}}_s \mathbf{E}_{q,s}^H \tag{58}$$

For unpolarized sources, we have $\tilde{\mathbf{C}}_s = \tilde{I}_s/2\mathbf{I}$, $\mathbf{C}_s = I_s/2\mathbf{I}$ as our coherencies, where the true and estimated Stokes I components are given by I_s and $\tilde{I}_s$, respectively. For the m-th source, assuming we have accurate fluxes for all other sources, the estimate is given as in (59).

$$\tilde{I}_m = (1+\varepsilon_m(\gamma))^2 I_m + \frac{1}{trace(\mathbf{E}_{p,m}\mathbf{E}_{q,m}^H)} \sum_{s=0,s\neq m}^{N-1} ((1+\varepsilon_s(\gamma))^2 - 1)I_s trace(\mathbf{E}_{p,s}\mathbf{E}_{q,s}^H) \tag{59}$$

The error in the flux estimate κ_m is given as in (60).

$$\kappa_m(\gamma) = ((1+\varepsilon_m(\gamma))^2 - 1)I_m + \frac{1}{trace(\mathbf{E}_{p,m}\mathbf{E}_{q,m}^H)} \sum_{s=0,s\neq m}^{N-1} ((1+\varepsilon_s(\gamma))^2 - 1)I_s trace(\mathbf{E}_{p,s}\mathbf{E}_{q,s}^H) \tag{60}$$

For idential beams, (60) has only real terms. We see that if $\varepsilon_m(\gamma) > 0$, then $\kappa_m(\gamma) > 0$ and if $\varepsilon_m(\gamma) < 0$, then $\kappa_m(\gamma) < 0$. We can use (60) to find the optimal value of elevation, γ_m, for a given source to estimate its flux with minimum error. This implies that we can find the optimal time for flux estimation of each source.

In order to proceed, we have to make some assumptions about the error in our beam model. At the zenith, we assume we have no error, or $\varepsilon_s(\gamma = \pi/2) = 0$ and at the horizon, we assume the error to be maximum. We shall assume a linear relationship, with maximum error of η at the horizon, as in (61).

$$\varepsilon_m(\gamma) = \frac{\eta}{\pi/2}(\pi/2 - \gamma), \quad 0 \leq \gamma \leq \pi/2 \tag{61}$$

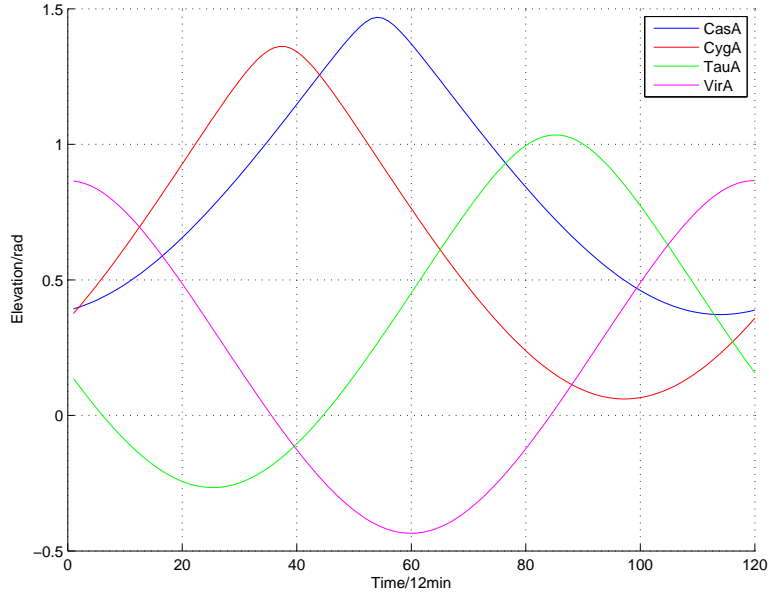Note that in (61), the elevation γ is unique to each source.

17

Figure 15: Elevation of the A Team during a 24 hour observation

We have given the elevations of the A Team sources during a 24 hour observation in Fig. 15. For the same observation, we have given the calculated value of (60) for Cyg A, Tau A, and Vir A, respectively in Fig. 16. This is for an observation with LBA dipoles at 60 MHz. The nominal flux values used were: Cas A (20000Jy), Cyg A (20000 Jy), Tau A (1800 Jy) and Vir A (3000 Jy).

Using Fig. 16, we can find the best time (or elevation) for flux estimation of each source. We have given the first results of this measurement in Figs. 17,18,19. Note that this is our initial result and we need to iterate to arrive at more accurate values.

10.2   Snapshot method

Estimation of flux and beam model can be simplified by using snapshot images. If we make snapshot images of the sky (say at 15 min intervals), the absolute positions of the sources on the dipole beam can be given as in Fig. (20) for a 24 hour observation. Note that we exploit the 90 degree rotation of the Y dipole w.r.t. X dipole to double the number of positions.

For each position in Fig. (20), we get a contraint on the beam model as well as the flux of the selected source. This can be given as in (62).

$$\|\widehat{\mathbf{C}} - \mathbf{E}(\boldsymbol{\theta})\mathbf{C}\mathbf{E}(\boldsymbol{\theta})^H\|^2 \tag{62}$$

In (62), we have parametrized the beamshape using an orthonormal basis (i.e., polar shapelets) where the parameters are given by $\boldsymbol{\theta}$. The estimated flux from the snapshot image is given as $\widehat{\mathbf{C}}$ and the true (unknown) flux is given by $\mathbf{C}$, in coherency form. By alternatively solving (62) for the beam and the fluxes, we can hopefully obtain a unique solution.

11   Acknowledgments

References

[1] Hamaker J.P., "Mathematical physical analysis of the generic dual dipole antenna," 2007

[2] Balanis C.A., "Antenna Theory (2nd Ed)," Wiley 1997.

[3] Lindmark B., and Nilsson M., "On the available diversity gain from different dual polarized antennas," *IEEE Jnl. on Selected Areas in Commun.,* vol. 19, no. 2, pp. 287-293, Feb. 2001.
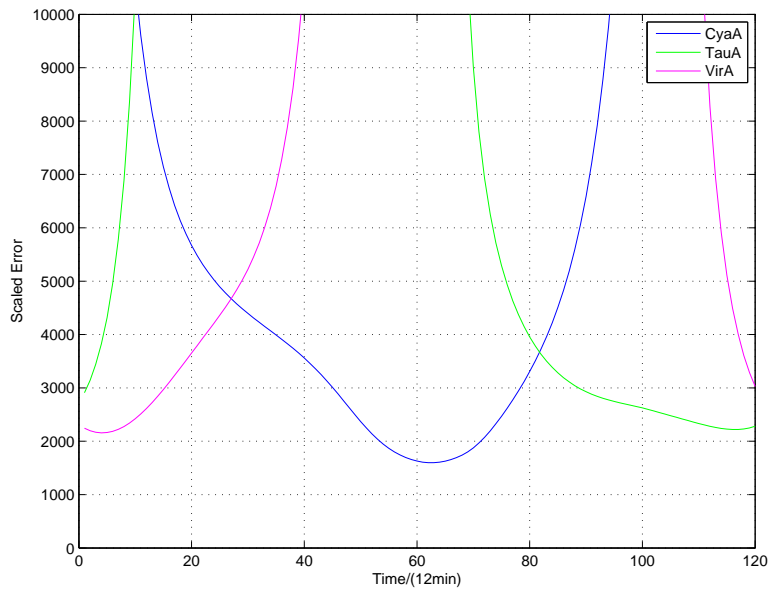
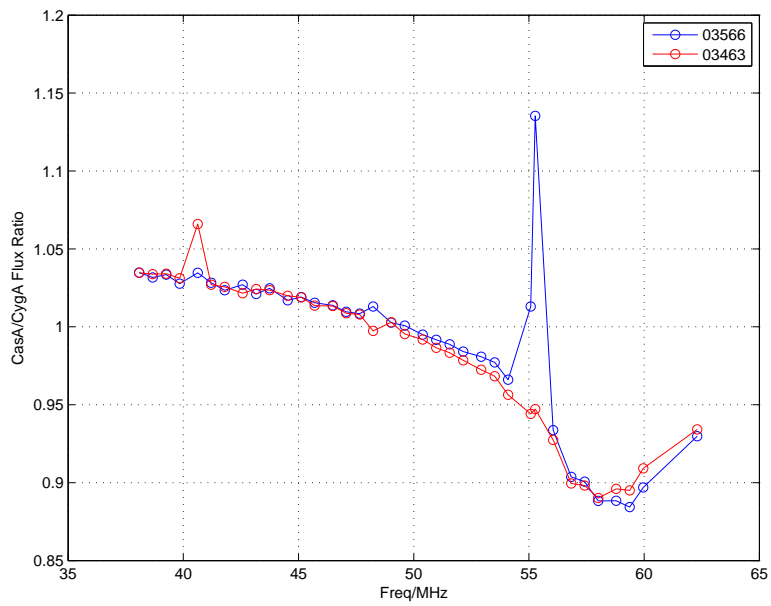Figure 16: Error in flux estimation

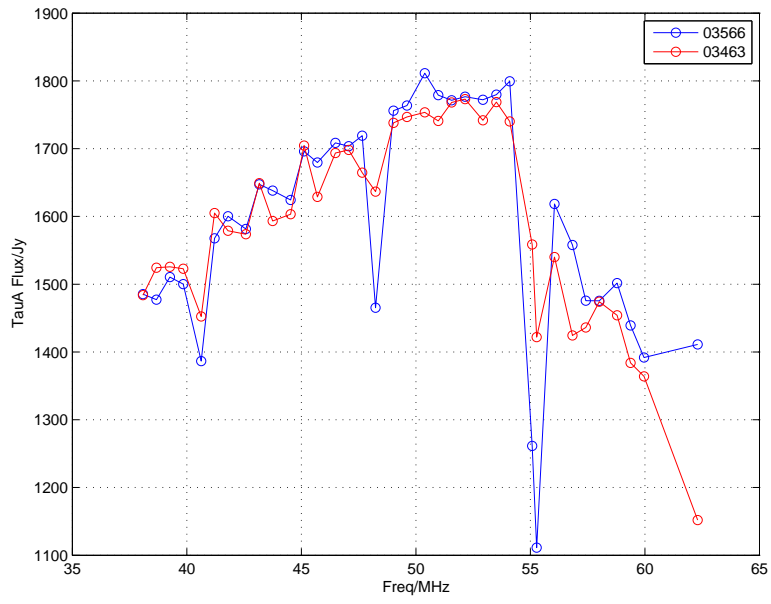

Figure 17: Flux ratio Cas A/Cyg A, with Cas A at 20000 Jy
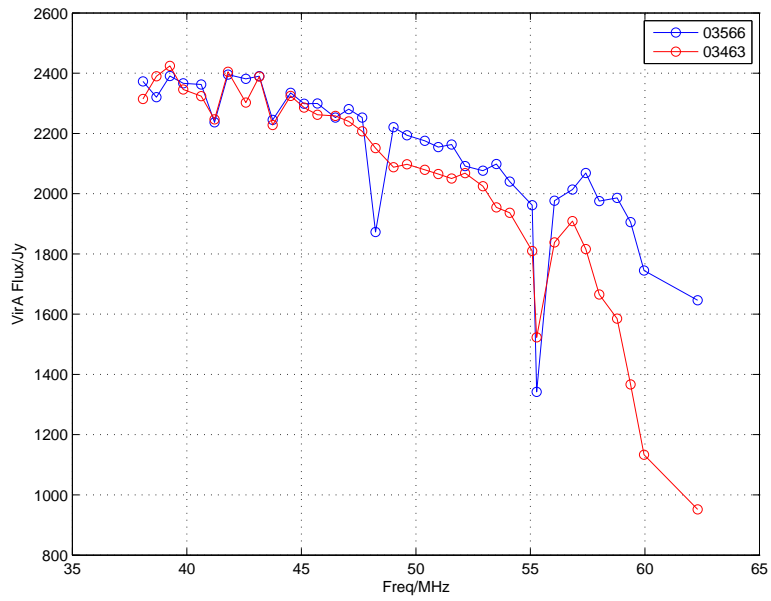
Figure 18: Flux of Tau A, with Cas A at 20000 Jy
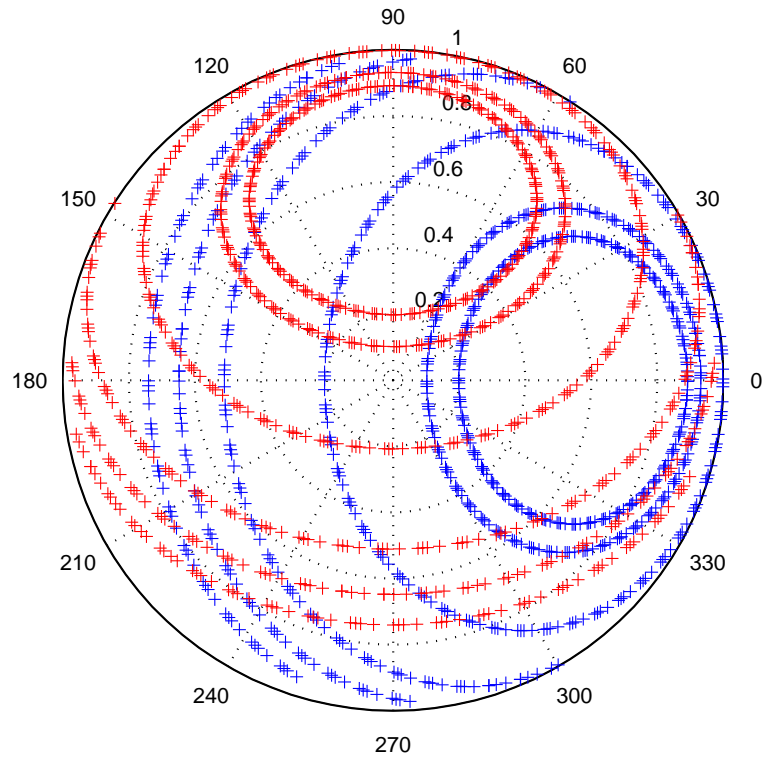

Figure 19: Flux of Vir A, with Cas A at 20000 Jy

20

Figure 20: Positions of the A-Team on the dipole beam for a 24 hour observation

[4] van Trees, H.L., "Detection, estimation and modulation theory, part IV: Optimum array processing," Wiley 2002.

[5] Lu, G., Korisch, I., Greenstein, L., and Spasojevic, P., "Antenna modelling using linear elements, with applications to UWB," IEEE Int. Symp. on Antennas and Propagation, vol. 3, pp. 2544-2547, Jun. 2004.